

Analysis of the mitigation strategies for COVID-19: from mathematical modelling perspective

S. M. Kassa^{†*}, H.J.B. Njagarah[†] and Y. A. Terefe[§]

[†]Department of Mathematics and Statistical Sciences,

Botswana International University of Science and Technology (BIUST), Private Bag 016, Palapye, Botswana

[§]Department of Mathematics and Applied Mathematics,

University of Limpopo, South Africa

Abstract

In this article, a mathematical model for the transmission of COVID-19 disease is formulated and analysed. It is shown that the model exhibits a backward bifurcation at $\mathcal{R}_0 = 1$ when recovered individuals do not develop a permanent immunity for the disease. In the absence of reinfection, it is proved that the model is without backward bifurcation and the disease free equilibrium is globally asymptotically stable for $\mathcal{R}_0 < 1$. By using available data, the model is validated and parameter values are estimated. The sensitivity of the value of \mathcal{R}_0 to changes in any of the parameter values involved in its formula is analysed. Moreover, various mitigation strategies are investigated using the proposed model and it is observed that the asymptomatic infectious group of individuals may play the major role in the re-emergence of the disease in the future. Therefore, it is recommended that in the absence of vaccination, countries need to develop capacities to detect and isolate at least 30% of the asymptomatic infectious group of individuals while treating in isolation at least 50% of symptomatic patients to control the disease.

Keywords: COVID-19; Disease model, Self-protection; Disease threshold; Backward bifurcation; Sensitivity Analysis; Mitigation strategy
2010 MSC: 92B05, 92D25, 92D30, 97M60

1 Introduction

A novel coronavirus, named a severe acute respiratory syndrome coronavirus 2 (SARS-CoV-2; previously known as 2019-nCoV), was identified as the infectious agent causing an outbreak of viral pneumonia in Wuhan, China, in December 2019 [43]. The World Health Organization (WHO) medical team codenamed the new outbreak caused by SARS-CoV-2 as “coronavirus disease 2019 (COVID-19)”. The infection is in the same category as the Severe Acute Respiratory Syndrome (SARS) which emerged in Southern China in 2002, spreading to up to 30 Countries, with a total of 8,098 cases

*Corresponding author: Email: kassas@biust.ac.bw

28 and claiming 774 lives [33]. COVID-19 is also in the same category as the Middle East Respiratory
29 Syndrome (MERS) which was first identified in Saudi Arabia in 2012, and ended up spreading to 27
30 countries around the world, reaching a total of 2,519 cases confirmed and claiming up to 866 lives
31 [41].

32 Since January 2020, an increasing number of cases confirmed to be infected with COVID-19
33 were detected outside Wuhan, and currently it has been spread all over the world. As of April 14,
34 2020, (08:26 GMT), COVID-19 had affected all continents including island nations (210 countries and
35 territories as well as 2 international conveyances), with the total number of cumulative infections
36 globally standing at 1,929,995 cases and 119,789 deaths [48], and the numbers is still increasing.

37 The major portal of entry of the virus in the body is the tissue lining the T-zones of the face
38 (including the nose, eyes and mouth). The infection is characterised by loss of the sense of smell (a
39 condition referred to as hyposmia/anosmia), taste and poor appetite. Although, such conditions
40 have been observed in COVID-19 patients, many carriers of the infection may not show any severe
41 symptoms like fever and cough but have hyposmia, loss of taste and loss of appetite.

42 Whereas knowledge of the virus dynamics and host response are essential for formulating
43 strategies for antiviral treatment, vaccination, and epidemiological control of COVID-19, estimation of
44 changes in transmission over time can provide insights into the epidemiological situation and help to
45 identify whether public health control measures are having a measurable effect [5, 35]. The analysis
46 from mathematical models may assist decision makers to estimate the risk and the potential future
47 growth of the disease in the population. Understanding the transmission dynamics of the infection
48 is crucial to design alternative intervention strategies [28]. In general, by approaching infectious
49 diseases from a mathematical perspective, we can identify patterns and common systems in disease
50 function, which would enable us to find some of the underlying structures that govern outbreaks and
51 epidemics.

52 Mathematical models that analyse the spread of COVID-19 have begun to appear in few published
53 papers and online resources [2, 9, 12, 28, 36]. However, there are several challenges to the use of
54 mathematical models in providing nearly accurate predictions at this early stage of the outbreak,
55 particularly in real time as it is difficult to determine many of the pathogen-based parameters through
56 mathematical models. The estimation of such parameters will require clinical observations and
57 “shoe-leather” epidemiology [30]. It is also possible for some of the parameters to be verified through
58 observation only at a later stage of the course of the epidemics. To get better predictions and to design
59 and analyse various alternative intervention strategies in the absence of such parameter values, one
60 needs to estimate them from existing epidemiological data.

61 Like many respiratory viruses, the novel coronavirus SARS-CoV-2 can be spread in tiny droplets
62 released from the nose and mouth of an infected person. As soon as the virus enters the body (either
63 through the mouth, nose or membrane of the eyes), it finds its way to the windpipe and then the
64 lungs. This viral attack is characterised by flu like symptoms, fever (body temperatures $> 38.3^{\circ}\text{C}$)
65 and dry cough at the initial stage of the infection. Once the virus gets into the lungs, it causes fibrosis
66 of the lungs leading to shortness of breath (or difficulty to breath) and severe pneumonia followed by
67 impaired functioning of the liver and acute kidney injury [20]. The virus is then released from the
68 infected individual when they cough, sneeze and when they touch their own nose or mouth. Some

69 part of the particles that are released through coughing or sneezing may land on clothing of other
70 people in close proximity, and surfaces around them while some of the smaller particles can remain
71 in the air for some times. In addition, some scientific evidences show that the virus can also be shed
72 for a longer time in faecal matters [45]. The virus survives on surfaces, fabrics, metals, plastics for
73 variable times. Recent report indicates that the virus can survive from shorter time (in the air) up to
74 2-3 days long on plastic and stainless-steel surfaces [39]. This implies that an uninfected individual
75 can also acquire the virus through contact of infected surfaces.

76 That means, there is a possibility for COVID-19 infection to spread from such contaminated
77 surfaces and objects to uninfected humans. Hence, including the proportion of indirect transmission
78 from the environment in the mathematical model structure is important to address this situation. We
79 note that the impact of environmental contamination and its role in the transmission of the disease is
80 not well studied in mathematical models developed so far.

81 Reinfection by the family of coronavirus is possible as it is indicated in [21, 50]. Even if it is not
82 yet well known how long it takes for a person who recovered from COVID-19 to loose immunity,
83 we can not overlook its impact at this stage. Therefore, when formulating a mathematical model for
84 COVID-19 dynamics, it is reasonable to consider a kind of Susceptible-Infected-Recovered-Susceptible
85 (SIRS) type of epidemiological model formulation.

86 So far there is no known curing medicine nor vaccine to combat the COVID-19 pandemic. The
87 available prevention mechanisms that are recommended by the WHO so far are also limited and their
88 effectiveness is not yet fully tested. The population level application of these preventive mechanisms
89 varies from region to region and from country to country. In some places, the protective measures
90 are employed voluntarily by individuals and in some other places governments impose some kind
91 of rules on the population to use strict social distancing and wearing face masks at public places.
92 However, the adherence to these rules is not uniform.

93 In the past, it has been witnessed that during the outbreak of infectious diseases, the human
94 population has been taking precautionary actions such that wearing masks, abstinence from risky
95 contacts, avoiding public transport means and increasing the uptake of vaccination (when available)
96 [14, 24, 32]. Behaviour change towards using preventive mechanisms by the population to protect
97 themselves from an infectious disease is assumed to be dependent on the way that the disease is
98 transmitted and its fatality. Individuals who have awareness about the disease and who decided to
99 use preventive mechanisms have less susceptibility than those without awareness and demonstrating
100 the usual risky behaviour.

101 A number of mathematical models have been proposed to analyse the effects of human behaviour
102 in the dynamics of infectious diseases (see [13, 15, 17, 22, 25, 26, 29, 32, 40], and the references therein).
103 In this paper, we follow the diffusion of innovation approach, which was proposed by Kassa and
104 Ouiniho [24]. In models of this approach, it is assumed that the perceived threat for the population is
105 the level of prevalence of the disease. However, for diseases with short time cycles, the prevalence
106 dependent awareness function looks non-realistic. Therefore, in this work we assumed that awareness
107 is driven by the magnitude of the incidence rate reported each day. That means, based on the diffusion
108 of innovation method one may consider the *perceived threat* for the population to be the incidence of
109 the disease.

110 At the beginning of the COVID-19 outbreak, a huge disparity has been observed in the use of
111 self-protective mechanisms and adherence to the advises given by public health agencies. In particular,
112 the people in some parts of Asia have fully embraced the measures while many in other parts of the
113 world were very much hesitant to use them. For example, wearing a face mask every day in public
114 appearance is like a ritual in most of the countries in South East Asia, while the same is considered
115 as a bad gesture in many of the other parts of the world [46] (even if it is now becoming a “normal
116 norm” also everywhere in the globe). One key difference between these societies and the people in
117 the West, is that the communities in the South East Asia have experienced similar disease outbreaks
118 before and the memories are still fresh and painful [46]. That means, recent history of a similar event
119 plays a role in behavioural change of the population specially at the beginning of the outbreak in
120 addition to the perceived threat from the disease.

121 Therefore, in this paper, we consider a mathematical model that takes into account

- 122 1. the transmission dynamics of COVID-19 similar to the SIRS model,
- 123 2. the contribution of the asymptomatic infectious individuals in the transmission dynamics of the
124 disease in the population,
- 125 3. the effect of indirect transmission of the disease through the environment,
- 126 4. behavioural change of individuals in the society to apply self-protective measures, and
- 127 5. the intensity of historical events from recent similar outbreaks.

128 By analysing the proposed mathematical model, the effect of each of these factors is investigated in
129 terms of their contribution in the control strategies of the disease.

130 The layout of this paper is as follows: The model is described and formulated in the next section.
131 Its qualitative analysis is presented in Section 3. Estimation of the parameters and the sensitivity
132 analysis of the reproduction number of the model with respect to involved parameters are discussed
133 in Section 4. Numerical simulations of the model with some assumed intervention scenarios are also
134 presented in this same section. Concluding remarks of the study are given in Sections 5.

135 **2 Model formulation**

136 In this section, we present a mathematical model for the transmission dynamics of COVID-19 which
137 spreads in a population. The susceptible individuals can be infected through either direct contact with
138 infectious individuals or indirect contact with novel coronavirus infected environment. The population
139 under consideration is grouped into disjoint compartments. Individuals who are susceptible to the
140 disease and without formal awareness about the prevention mechanisms or who did not decide to
141 use any one of them are grouped in the S class. Individuals who are susceptible but are aware of
142 about and decided to apply any of the existing protective mechanisms after receiving public health
143 information on how to protect themselves from the novel coronavirus infection are placed in the S_e
144 class. COVID-19 infected individuals who are asymptomatic and symptomatic are grouped in classes
145 C and I , respectively. Some studies consider the asymptomatic class as the “exposed” class (see for
146 instance [9]). But since the individuals in this group are known to be infectious and some of them
147 also recover from the disease without going through the I group [8], we used a name “carrier” to

148 avoid confusion. The R class contains the recovered individuals from COVID-19. Finally, E denotes
 149 the amount of the novel coronavirus pathogen that contaminates the environment due to shedding
 150 by COVID-19 infectious individuals. In the analysis of the model, we intentionally excluded the
 151 actual exposed class for mathematical simplicity. However, a 5 days incubation period is taken into
 152 consideration in the numerical simulation part of this paper.

Variables	Description
S	Susceptible population.
S_e	Susceptible individuals who are educated to prevent the disease.
C	Carriers individuals (infected & infectious but asymptomatic).
I	Infected individuals (symptomatic).
R	Recovered individuals.
E	Contaminated surfaces or objects in the environment.

Table 1: Description of the model variables

153 By combining the direct and indirect way of transmissions, the force of infection is assumed to
 154 have the form

$$\lambda = \beta_1 \frac{I + \nu C}{N} + \beta_2 \frac{E}{E + K'} \quad (2.1)$$

155 where $N = S + S_e + C + I + R$ and K is the concentration of the novel coronavirus in the environment
 156 which increases 50% chance of triggering the disease transmission.

157 The proposed flow diagram for the transmission dynamics of COVID-19 is depicted in Figure 1
 158 while the description of each of the state variables is given in Table 1.

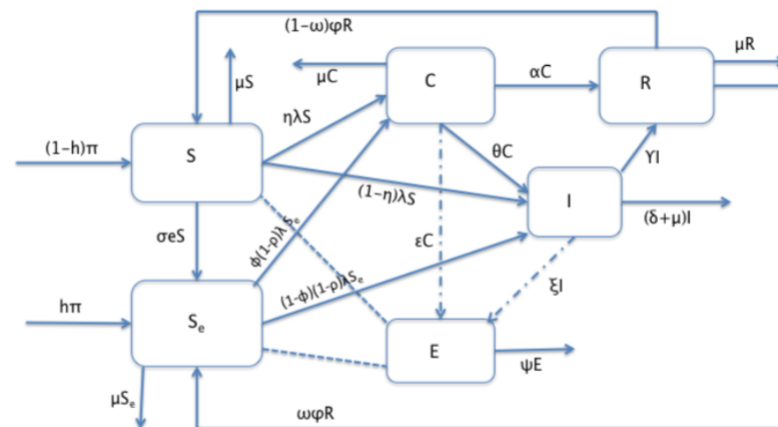


Figure 1: Schematic diagram of the proposed model

159 The dynamics of the pandemic is described by using the following system of differential equations
 160 (see Table 2 for the description of the involved parameters):

$$\begin{aligned}
 S' &= (1 - h)\pi - (\lambda + \sigma e + \mu)S + (1 - \omega)\varphi R, \\
 S_e' &= h\pi + \sigma eS - ((1 - \rho)\lambda + \mu)S_e + \omega\varphi R, \\
 C' &= \eta\lambda S + \phi(1 - \rho)\lambda S_e - (\theta + \alpha + \mu)C, \\
 I' &= (1 - \eta)\lambda S + (1 - \phi)(1 - \rho)\lambda S_e + \theta C - (\gamma + \mu + \delta)I, \\
 R' &= \alpha C + \gamma I - (\varphi + \mu)R, \\
 E' &= \epsilon C + \xi I - \psi E,
 \end{aligned}
 \tag{2.2}$$

161 where

$$e(\lambda) = \frac{\lambda^n}{\lambda_0^n + \lambda^n}
 \tag{2.3}$$

with λ_0 is the value of the force of infection corresponding to the threshold infectivity in which individuals start reacting swiftly (that means, the point at which the behaviour change function changes its concavity). We appended the following nonnegative initial conditions with the system (2.2):

$$S(0) = S_0, S_e(0) = S_{e_0}, C(0) = C_0, I(0) = I_0, R(0) = R_0, \text{ and } E(0) = E_0.$$

Parameters	Description
Π	Rate of recruitment to the susceptible individuals
h	Fraction of recruitment to the S_e class because of past disease history
σ	Rate of dissemination of information about the disease in the population
η	Fraction of infected susceptible individuals who become carriers
ϕ	Fraction of 'educated' individuals who get infected and become carriers
ρ	Average effectiveness of existing self-preventive measures
α	Rate of recovery for carrier individuals
θ	Rate of transfer of carrier individuals to the sick class
ϵ	Shedding rate from the C class to the environment
γ	Rate of recovery for the sick class
δ	Death rate due to coronavirus
ξ	Shedding rate from the I class to the environment
ψ	Virus decay rate from the environment
β_1	Rate of disease transmission directly from humans
β_2	Rate of disease transmission from the environment
K	The pathogen concentration in the environment that yields 50% of chance for a susceptible individual to catch the viral infection from the environment
ν	Modification parameter (transmission of C relative to I)
φ	Rate of losing immunity after recovery
μ	Natural death rate
ω	Fraction of recovered individuals moving into the S_e class after losing immunity

Table 2: Description of the model parameters

3 Analysis of the model

In this section, we study the quantitative and qualitative analysis of the model system Eq. (2.2).

3.1 Well-posedness

We begin by determining the biologically feasible set for the model (2.2). The following theorem implies that the solutions of (2.2) are nonnegative and bounded from above, provided that the initial conditions are nonnegative.

Theorem 3.1 Equation (2.2) defines a dynamical system on Ω , where

$$\Omega = \left\{ (S, S_e, C, I, R, E) \in \mathbb{R}_+^6 : 0 \leq S + S_e + C + I + R = N \leq \frac{\pi}{\mu}, 0 \leq E \leq \frac{(\epsilon + \xi)\pi}{\mu\psi} \right\}. \quad (3.1)$$

Proof: The proof of this Theorem is outlined in Appendix A

3.2 Asymptotic stability of the disease-free equilibrium

To determine the equilibrium solutions, we set the right-hand side of (2.2) equal to zero and obtain

$$\begin{aligned} (1-h)\pi - (\lambda + \sigma e + \mu)S + (1-\omega)\varphi R &= 0, \\ h\pi + \sigma e S - ((1-\rho)\lambda + \mu)S_e + \omega\varphi R &= 0, \\ \eta\lambda S + \phi(1-\rho)\lambda S_e - (\theta + \alpha + \mu)C &= 0, \\ (1-\eta)\lambda S + (1-\phi)(1-\rho)\lambda S_e + \theta C - (\gamma + \mu + \delta)I &= 0, \\ \alpha C + \gamma I - (\varphi + \mu)R &= 0, \\ \epsilon C + \xi I - \psi E &= 0. \end{aligned} \quad (3.2)$$

Then, the disease-free equilibrium (DFE) is obtained to be

$$\mathcal{E}_0 = \left(\frac{(1-h)\pi}{\mu}, \frac{h\pi}{\mu}, 0, 0, 0, 0 \right). \quad (3.3)$$

The basic reproduction number, which is very important for the qualitative analysis of the model, is determined here below by using the method of the next generation matrix used in [11, 38]. For the model under consideration, using the notation $X = (C, I, E)$, we have the vector functions

$$\mathcal{F}(X) = \begin{pmatrix} \eta\lambda S + \phi(1-\rho)\lambda S_e \\ (1-\eta)\lambda S + (1-\phi)(1-\rho)\lambda S_e \\ 0 \end{pmatrix},$$

and

$$\mathcal{V}(X) = \begin{pmatrix} k_1 C \\ -\theta C + k_2 I \\ -(\epsilon C + \xi I) + \psi E \end{pmatrix},$$

179 with $k_1 = \theta + \alpha + \mu$ and $k_2 = \gamma + \mu + \delta$ represent the rates at which the disease compartments increase
 180 and decrease in size due to the infection, respectively. Then the next generation matrix is

$$\mathbf{B} = J_{\mathcal{F}}(J_{\mathcal{V}})^{-1}, \quad (3.4)$$

181 where

$$182 \quad J_{\mathcal{F}}(\mathcal{E}_0) = \begin{pmatrix} v\beta_1 p & \beta_1 p & \frac{\beta_2 \pi}{\mu K} p \\ v\beta_1 q & \beta_1 q & \frac{\beta_2 \pi}{\mu K} q \\ 0 & 0 & 0 \end{pmatrix},$$

183 and

$$184 \quad J_{\mathcal{V}}(\mathcal{E}_0) = \begin{pmatrix} k_1 & 0 & 0 \\ -\theta & k_2 & 0 \\ -\epsilon & -\zeta & \psi \end{pmatrix}.$$

185 where $p = \eta(1 - h) + \phi(1 - \rho)h$, and $q = (1 - \eta)(1 - h) + (1 - \phi)(1 - \rho)h$. Here, it is not difficult to
 186 show that

$$187 \quad J_{\mathcal{V}}^{-1}(\mathcal{E}_0) = \begin{pmatrix} \frac{1}{k_1} & 0 & 0 \\ \frac{\theta}{k_1 k_2} & \frac{1}{k_2} & 0 \\ \frac{1}{k_1 \psi} \left(\epsilon + \frac{\theta \zeta}{k_2} \right) & \frac{\zeta}{k_2 \psi} & \frac{1}{\psi} \end{pmatrix}.$$

188 The basic reproduction number denoted by \mathcal{R}_0 is defined as the average number of secondary
 189 cases produced in a completely susceptible population by a typical infected individual during its
 190 entire period of being infectious [11, 38]. Mathematically, \mathcal{R}_0 is the spectral radius of \mathbf{B} in Eq. (3.4)
 191 and after further simplification, we obtain

$$\mathcal{R}_0 = \beta_1 \left[\frac{p}{k_1} \left(v + \frac{\theta}{k_2} \right) + \frac{q}{k_2} \right] + \frac{\beta_2 \pi}{\mu \psi K} \left[\frac{p}{k_1} \left(\epsilon + \frac{\theta \zeta}{k_2} \right) + \frac{q \zeta}{k_2} \right]. \quad (3.5)$$

192 The next result is a direct application of Theorem 2 in [38].

193 **Theorem 3.2** *The DFE \mathcal{E}_0 of the model (2.2) is locally asymptotically stable whenever $\mathcal{R}_0 < 1$ and unstable if*
 194 *$\mathcal{R}_0 > 1$.*

195 The epidemiological implication of Theorem 3.2 is that the transmission of COVID-19 can be controlled
 196 by having $\mathcal{R}_0 < 1$ if the initial total numbers in each of the subpopulation involved in Eq.(2.2) are in
 197 the basin of attraction of \mathcal{E}_0 . To ensure that eliminating the disease is independent of the initial size of
 198 the subpopulation, the disease-free equilibrium must be globally asymptotically stable when $\mathcal{R}_0 < 1$.
 199 This is what we present here below.

200 **Theorem 3.3** *The model (2.2) undergoes a backward bifurcation at $\mathcal{R}_0 = 1$ when the parameters satisfy the*
 201 *condition*

$$\frac{DH + GJ}{(p + qF)L} \geq 1, \quad (3.6)$$

202 where

$$\begin{aligned}
 A &= \frac{\mu\psi k_1 K \left[\beta_1 \left(\frac{p\theta}{k_1 k_2} + \frac{q}{k_2} \right) + \frac{\beta_2 \pi}{\mu\psi K} \left(\frac{p\theta\zeta}{k_1 k_2} + \frac{q\zeta}{k_2} \right) \right]}{p(\mu\psi\beta_1 K + \zeta\beta_2 \pi)}, \\
 D &= \frac{1}{\mu} \left[\frac{(1-\omega)\varphi(\alpha + \gamma A)}{k_3} - (1-h) \left(\beta_1(v + A) + \frac{\beta_2 \pi}{\mu\psi K} (\epsilon + \zeta A) \right) \right], \\
 F &= \frac{p(\mu\psi\beta_1 K + \zeta\beta_2 \pi)}{q(v\mu\psi\beta_1 K + \epsilon\beta_2 \pi) + \mu\psi\theta K} A \\
 G &= \frac{1}{\mu} \left[\frac{\omega\varphi}{k_3} (\alpha + \gamma A) - (1-\rho)h \left(\beta_1(v + A) + \frac{\beta_2 \pi}{\mu\psi K} (\epsilon + \zeta A) \right) \right] \\
 H &= \frac{\mu\beta_1}{\pi} (v + A) (\eta - p + F(1 - \eta - q)) + \frac{\beta_2 (\epsilon + \zeta A)}{\psi K} (\eta + F(1 - \eta)) \\
 J &= \frac{\mu\beta_1}{\pi} (v + A) (1-h) \left[(-\eta + \phi(1-\rho)) + F(- (1-\eta) + (1-\phi)(1-\rho)) \right] \\
 &\quad + \frac{(1-\rho)\beta_2 (\epsilon + \zeta A)}{\psi K} (\phi + F(1-\phi)) \\
 L &= \frac{\mu\beta_1}{\pi} \left(v + A(1 + v + A) + \frac{\alpha + \gamma A}{k_3} (v + A) \right) + \frac{\beta_2 \pi}{\mu} \left(\frac{\epsilon + \zeta A}{\psi K} \right)^2.
 \end{aligned}$$

203 The proof of Theorem 3.3 is carried out using the center manifold theory in [6] and is given in
 204 Appendix B

205

206 In the above theorem (Theorem 3.3), if the reinfection parameter $\varphi = 0$, we can observe that both
 207 D and G are negative. Hence, Eq. (3.6) can not be true. In this case, we give below a Theorem which
 208 asserts the global stability of the DFE of the model.

209 **Theorem 3.4** *The disease-free equilibrium of system (2.2) in the case when $\varphi = 0$ is globally asymptotically*
 210 *stable for $\mathcal{R}_0 < 1$.*

211 **Proof:** To prove the theorem for the case $\varphi = 0$, we use Kamgang-Sallet Stability Theorem stated in
 212 [23]. Let $X = (X_1, X_2)$ with $X_1 = (S, S_e, R) \in \mathbb{R}^3$ and $X_2 = (C, I, E) \in \mathbb{R}^3$. Then the system (2.2) can
 213 be written as

$$\dot{X}_1 = A_1(X)(X_1 - X_1^*) + A_{12}(X)X_2, \quad (3.7)$$

$$\dot{X}_2 = A_2(X)X_2, \quad (3.8)$$

214 where $X_1^* = \left(\frac{(1-h)\pi}{\mu}, \frac{h\pi}{\mu}, 0 \right)$,

$$215 \quad A_1(X) = \begin{pmatrix} -\mu & 0 & 0 \\ 0 & -\mu & 0 \\ 0 & 0 & -\mu \end{pmatrix},$$

$$216 \quad A_{12}(X) = \begin{pmatrix} -k_4 \frac{v\beta_1}{N} S & -k_4 \frac{\beta_1}{N} S & -k_4 \frac{\beta_2}{E+K} S \\ k_5 \frac{v\beta_1}{N} & k_5 \frac{\beta_1}{N} & k_5 \frac{\beta_2}{E+K} \\ \alpha & \gamma & 0 \end{pmatrix},$$

217 and

$$218 \quad A_2(X) = \begin{pmatrix} \frac{v\beta_1}{N}k_6 - k_1 & \frac{\beta_1}{N}k_6 & k_6\frac{\beta_2}{E+K} \\ \frac{v\beta_1}{N}k_7 + \theta & \frac{\beta_1}{N}k_7 - k_2 & \frac{\beta_2}{E+K}k_7 \\ \epsilon & \zeta & -\psi \end{pmatrix}.$$

219 with $k_4 = 1 + \frac{\sigma\lambda^{n-1}}{\lambda^n + \lambda_0^n}$, $k_5 = \frac{\sigma\lambda^{n-1}}{\lambda^n + \lambda_0^n}S - S_e$, $k_6 = \eta S + \phi S_e$ and $k_7 = (1 - \eta)S + (1 - \phi)S_e$.

220 We show that the five sufficient conditions of Kamgang-Sallet Theorem (in [23]) are satisfied as
221 follows.

- 222 1. The system (2.2) is a dynamical system on Ω . This is proved in Theorem 3.1.
- 223 2. The equilibrium X_1^* is GAS for the subsystem $\dot{X}_1 = A_1(X_1, 0)(X_1 - X_1^*)$. This is obvious from
224 the structure of the involved matrix.
- 225 3. The matrix $A_2(X)$ is Metzler (i.e., all the off-diagonal elements are nonnegative) and irreducible
226 for any given $X \in \Omega$.
- 227 4. There exists an upper-bound matrix \bar{A}_2 for the set

$$\mathcal{M} = \{A_2(X) : X \in \Omega\}.$$

227 Indeed,

$$228 \quad \bar{A}_2 = \begin{pmatrix} v\beta_1 p - k_1 & \beta_1 p & \frac{\beta_2}{K} p \\ v\beta_1 q + \theta & \beta_1 q - k_2 & \frac{\beta_2}{K} q \\ \epsilon & \zeta & -\psi \end{pmatrix}$$

229 with $p = (1 - h)\eta + h\phi$ and $q = (1 - h)(1 - \eta) + h(1 - \phi)$ is an upper-bound for \mathcal{M} .

- 230 5. For $\mathcal{R}_0 \leq 1$ in Eq. (3.5)

$$\alpha(\bar{A}_2) = \max \{Re(\lambda) : \lambda \text{ eigenvalue of } \bar{A}_2\} \leq 0.$$

230 Hence, by the Kamgang-Sallet Stability Theorem [23], the disease-free equilibrium is globally
231 asymptotically stable for $\mathcal{R}_0 < 1$. \square

232 The reality behind Theorem 3.4 is that, if immunity is permanent ($\varphi = 0$), coronavirus will be
233 effectively controlled in the community if \mathcal{R}_0 can be brought to a value less than unity.

234 4 Numerical Simulations and Discussion

235 4.1 Estimation of parameters from data and literature

236 The novel coronavirus being a new strain of corona viruses, information about the dynamics of the
237 infection is still evolving. Biological studies of parameter values describing the vital dynamics of the
238 infection are still ongoing as more laboratory test become available. Although some studies have been
239 done on the early dynamics of the disease most especially on data from Wuhan, extensive reading
240 reveals that some of the disease dynamics parameters are highly variable and some process are not
241 fully explored. In this work, we use new cases data from Hubei Province of China extracted from

242 WHO situation reports 1-57 [43], i.e. for the period January 21, 2020 to March 17, 2020. We ought to
243 fit the proposed model to the extracted data and estimate the unknown parameters.

244 The total population of Hubei province was estimated as 59.2 million. The life expectancy of
245 Hubei province varies depending on the area of dwelling (i.e urban or rural) as well as gender [44].
246 For urban dwellers, the average life expectancy is estimated to be 75.68 years (with an average being
247 73.72 years for men and 77.79 years for women). The life expectancy of China of the year 2019 was
248 estimated to be 76.79 years where as that for the year 2020 is estimated as 76.96 years. [31]. Owing to
249 the negligible difference in the provincial and Country wide value, we use the Country life expectancy
250 for the year 2019 which gives an average mortality rate of $\mu = 3.57 \times 10^{-5}$ per day. The recruitment
251 rate is thus given as $\pi = \mu \times N_0$, where N_0 is taken to be the total population size, 59.2 million.

252 The average time period taken for symptoms to appear after exposure is observed to vary
253 considerably with a range between 2-14 days [7], 2-24 days [47], with some outliers going to up to 27
254 days. The observed median incubation period was nearly 5 days [16]

255 The time to recovery from the onset of symptoms varies depending on the seriousness of the
256 infection with individuals presenting mild illness observed to recover in an average period of 2
257 weeks while those presenting serious/critical illness recovering in about 3 to 6 weeks. For our
258 parameter estimate simulations we consider a nominal value of 0.0476 day^{-1} (corresponding to 3
259 weeks) estimated from an interval (0.0238, 0.0714). We note that a patient is considered recovered: (1)
260 if two swab tests taken in a time interval of at least 24 hours both test negative, (2) if the time taken
261 for after the end of the respiratory symptoms and fever is at least 72 hours.

262 The waning of the immunity after recovery is estimated to range between 4 months to 1 year,
263 which gives an interval for φ as (0.00274, 0.00824) day^{-1} . For our simulation, we consider a nominal
264 value of $\varphi = 0.00274 \text{ day}^{-1}$ (approximately one year). We propose that at the end of the epidemic, at
265 least 20 – 65% of the recovering population will learn from the experiences during the infection and
266 even when the acquired immunity wanes, such individuals will become susceptible individuals with
267 past history/knowledge of the disease.

268 The rate of recovery for the symptomatic individuals (γ) in Wuhan varied considerably but
269 majority of individuals who recovered from the virus were discharged from hospital after $2\frac{1}{2}$ weeks
270 [4]. However, the patients in Wenzhou-China stayed in hospital for 27 days (0.037 per day) on average.
271 In the model fitted on the early trends data from Wuhan-China [27], the recovery rate obtained for
272 symptomatic cases was 0.0897 per day (accounting for 10 days to recovery). The rate of recovery (α)
273 for carrier individuals is expected to be higher [9].

274 According to the WHO situation report [42], it is estimated that up to 80% of COVID-19 cases
275 are asymptomatic or show mild symptoms, 15% show severe symptoms and up-to 5% end up with
276 critical infection and require oxygen or a ventilator. The proportion of individuals who do not show
277 symptoms or have mild symptoms can be as high as 94% [18]. For our model fitting, we use a range
278 of (0.65, 0.86) for both η and ϕ with selected initial values within the prescribed interval.

279 Although Hubei province was put on a lockdown on January 23, 2020, the first major decline in
280 the number of new confirmed cases was only observed on February 20, 2020 (Situation report 31 [43]),
281 approximately 1 month after the lockdown was imposed. From February 14, 2020, the method of
282 identification of new cases was revised to include both cases confirmed through laboratory test and

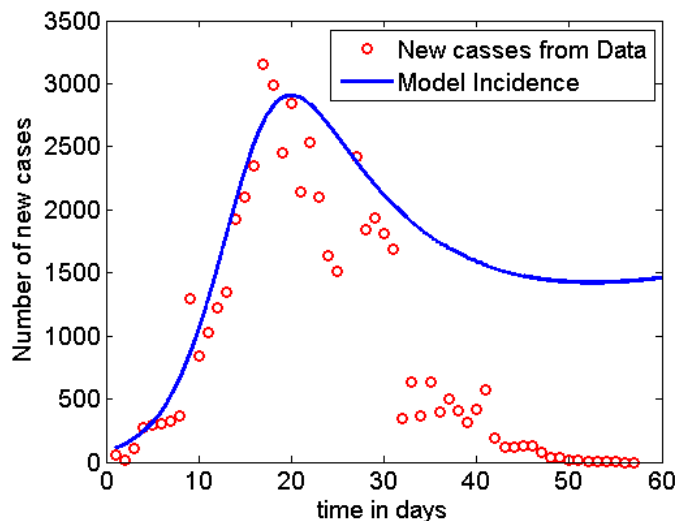


Figure 2: Model fit to the data

283 clinical observation. As such there was an observed spike in the number of new cases on February
284 14, 2020 of 4823 compared to 1508 cases (reported on February 13, 2020) and 2420 cases (reported
285 February 15, 2020).

286 Applying the above described set of assumptions in the bound for some of the parameters, we
287 optimize the model output to fit the daily new cases data reported for the Hubei province, China.
288 The parameter values that best fit to the incidence data is given in Table 3. Figure 2 shows the plot of
289 the reported new-case data together with the incidence of the disease obtained from the model. As
290 we can observe from the graph, the model slightly overestimates the reported data except for the two
291 highest points. In addition, since our model does not assume any control measure at this stage while
292 the reported data after the 31st day may represent the effect of the strict lockdown measure taken by
293 the authorities, the parameters estimated seem to give a good result. When we calculate the value of
294 \mathcal{R}_0 from Eq. (3.5) using the estimated parameters given in Table 3, we obtain $\mathcal{R}_0 \approx 2.91$, which is
295 within the range of values reported in [10, 49].

296 4.2 Sensitivity analysis

297 We examine the sensitivity of \mathcal{R}_0 to variations in parameter values and establish the significance of
298 the sensitivity indices. We used the Latin hypercube Sampling (LHS) scheme, which is an efficient
299 stratified Monte Carlo sampling that allows for simultaneous sampling of the multi-dimensional
300 parameter space [19]. For each run, 1000 simulations were done and Partial Rank Correlation
301 Coefficients (PRCCs) [1] calculated between each of the selected input parameters and the disease
302 threshold. The PRCCs indicate the degree of effect each parameter has on the outcome, which in
303 this case is the disease threshold. The sign of the PRCC identifies the specific qualitative relationship
304 between the input parameter and the output variable. The positive value of the PRCC of the variables
305 implies that when the value of the input parameter increases, the future number of cases will also

Parameter	Description	Range	Nominal Value	Source
Π	Persons day ⁻¹		$\mu \times N_0$	Assumed
β_1	Contacts day ⁻¹	(0.24, 0.275)	0.275	Fitted
β_2	Contacts day ⁻¹	(0.001, 0.028)	0.001006082	Fitted
h	proportion	(0.1, 0.65)	0.59996	Fitted
ν	Relative value	(1.1 – 3)	2.662830741	Fitted
K	No. of pathogens	(100-10 ⁷)	2091775	Fitted
σ	Intensity day ⁻¹	(0.2, 0.65)	0.649996150	Fitted
ϕ	Proportion	(0.65, 0.86)	0.8671	Fitted
η	Proportion	(0.65, 0.86)	0.650286467	Fitted
ρ	Proportion	(0.10, 0.15)	0.149999732	Fitted
α	day ⁻¹	(0.04, 0.075)	0.074999946	Fitted
θ	day ⁻¹	(0.1, 0.25)	0.249999979	Fitted
ε	Pathogens person ⁻¹ day ⁻¹	(0.098, 0.33)	0.101989917	Fitted
γ	day ⁻¹	(0.025, 0.05)	0.049999999	Fitted
ζ	Pathogens person ⁻¹ day ⁻¹	(0.135, 0.673)	0.431477395	Fitted
δ	day ⁻¹	(0.006, 0.11)	0.11	Fitted
ψ	day ⁻¹	(0.14 – 1)	0.2842	Fitted
μ	day ⁻¹		3.57×10^{-5}	[44]
φ	day ⁻¹	(0.00274, 0.00824)	0.00274	Fitted
ω	Proportion	(0.2, 0.65)	0.633695	Fitted

Table 3: Nominal values and ranges of parameters values.

306 increases. On the other hand, processes underlying the parameters with negative PRCCs have a
 307 potential to contain of the number of cases when enhanced. The results of sensitivity analysis
 308 are indicated in Figure 3(a) and the box plot (Figure 3(b)) gives the five-number summary for the
 computed disease threshold value from the sampled parameter space.

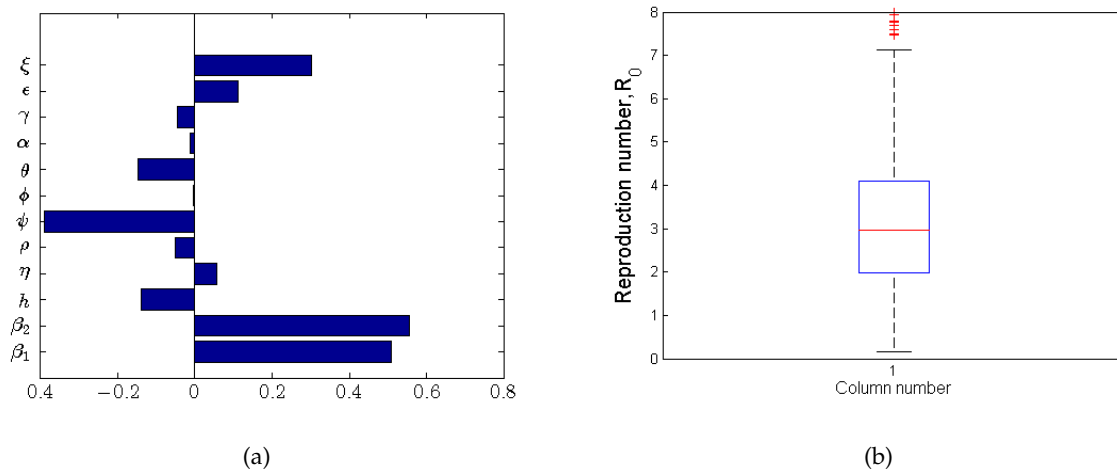


Figure 3: Partial Rank Correlation Coefficients (PRCCs) for a selected range of model parameters in Table 3. The processes underlying the parameters β_1 , β_2 , ϵ and ξ have the greatest potential of making the epidemic worse if increased, whereas processes described by ψ and h have the greatest potential of containing the epidemic when enhanced.

309

310 The processes described by parameters β_1 , β_2 , ϵ and ξ with the greatest positive PRCCs have the
 311 greatest potential of worsening pandemic when increased. On the other hand, parameters (h and ψ)
 312 with negative PRCCs have the greatest potential in helping contain the infection when maximised.
 313 In this respect, we note that increasing social/physical distancing directly reduces β_1 as this lowers
 314 the likelihood of a susceptible individual getting in contact with a potentially infected individual. In
 315 addition, practising good hygiene (such as regularly washing hands, using sanitisers to disinfect the
 316 infected environment and avoiding touching the T-zones of the face) is associated with lowering the
 317 likelihood of contracting the virus from infected surfaces. Anything contrary to the above increases
 318 the likelihood of getting the infection through the two aforementioned routes. We further note that
 319 practising good hygiene also involves the infected individuals reducing the shedding of the virus into
 320 the environment. It is evident from the results in figure 3 and Table 4 that reducing the rate at which
 321 the virus is shed into the environment is significant in reducing the severity of the problem.

322 From the five number summary of the results in Figure 3(b), the lower quartile of the computed
 323 values of R_0 is about 2, the median around 2.9 and the upper quartile of about 4. The obtained value
 324 of R_0 is within the range of 3.11 (95%CI, 2.39 – 4.13) obtained in the early studies in [34]. We note that
 325 for a selected combination of underlying processes much higher values of R_0 can be obtained, which
 326 is an indication of possible worsening of the situation. In a similar way, we observe that for particular
 327 underlying processes (a selected combination of parameters) the value of R_0 can be reduced to values
 328 below one.

329 As indicated in [1], we note that although some parameters in the model may have very small
 330 magnitudes of PRCCs (non-monotonically related to the disease threshold output), they may still
 331 produce sizeable changes in the disease burden. To identify the most important parameters in
 332 containing or aggravating the epidemic, we computed p-values for the simulated parameters using
 333 Fisher’s Transformation [1]. We note that the computed PRCCs are bounded between the interval
 334 $[-1, 1]$. For this matter, some sampling distribution of variables that are highly correlated is skewed.
 335 The Fisher’s Transformation $\rho(r) = 0.5 \log\left(\frac{1+r}{1-r}\right)$ is used to transform the skew distribution to a
 336 normal distribution and then compute p-values for each of the parameters based on the PRCCs [1].
 The PRCCs for the parameters together with their corresponding p-values are indicated in Table 4.

Variable	PRCC	P-value	Significance?
β_1	0.108132611	1.566×10^{-3}	TRUE
β_2	0.706803546	0.0000000	TRUE
h	-0.081725771	2.022×10^{-2}	TRUE
η	0.003556638	0.9110	FALSE
ρ	-0.037485329	0.3186	FALSE
ψ	-0.4787134264	0.00000	TRUE
ϕ	0.004377062	0.9110	FALSE
θ	-0.060636753	0.09703	FALSE
α	-0.021180254	0.607	FALSE
γ	-0.045896543	0.223	FALSE
ε	0.159616950	1.289132×10^{-06}	TRUE
ξ	0.359785405	0.000000	TRUE

Table 4: Parameter PRCC significance (FDR Adjusted P-values)

337
 338 We carry out pairwise comparison of the significant parameters (whose p-values are less than
 339 0.05, see Table 4) to ascertain whether the process described by such parameters are different. We
 340 computed the p-values for the different pairs of significant parameters while accounting for the false
 341 discovery rate (FDR) adjustment and the results are given in Table 5.

	β_1	β_2	h	ψ	ε	ξ
β_1		0	2.347×10^{-5}	0	0.2443	2.642×10^{-9}
β_2			0	0	0	0
h				0	8.647×10^{-8}	0
ψ					0	0
ε						1.942×10^{-6}
ξ						

Table 5: Pairwise PRCC Comparisons (FDR Adjusted P-values)

342 The major question posed at this point is: Are the different pairs of significant parameters
 343 different after FDR adjustment? Based on the FDR adjusted p-values in Table 5, the compared pair of
 344 parameters are rendered to be different if their p-value is less than 0.05 and not different otherwise.

345 We summarise our results in Table 6, where “TRUE” indicates that the compared parameters are significantly different and “FALSE” indicating that the parameters are not significantly different.

	β_1	β_2	h	ψ	ε	ζ
β_1		TRUE	TRUE	TRUE	FALSE	TRUE
β_2			TRUE	TRUE	TRUE	TRUE
h				TRUE	TRUE	TRUE
ψ					TRUE	TRUE
ε						TRUE
ζ						

Table 6: Are the parameters different after FDR adjustment?

346

347 We observe that the more sensitive parameters are also significantly different (see Table 6) except
 348 for the $\beta_1 - \varepsilon$ pair which may not necessarily be related.

349 We examine effect of variation of the sensitive parameters on the reproduction number (\mathcal{R}_0). The
 350 results of the variation of parameters with more negative PRCCs are indicated in the bar graphs in
 Figure (4).

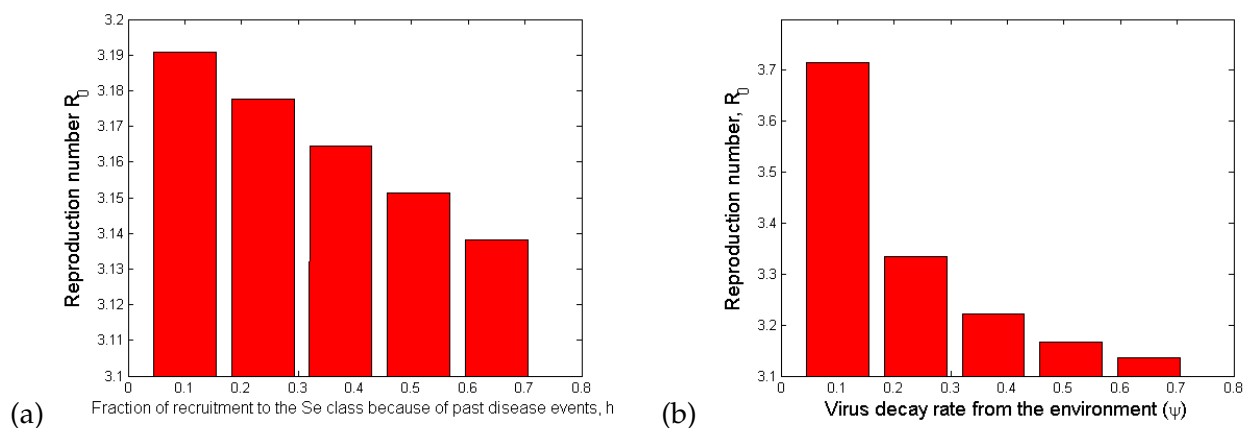


Figure 4: Bar plots showing the effect of the most sensitive parameters to \mathcal{R}_0 : (4(a)) Fraction of recruitment to the Se class because of past disease events; (4(b)) Virus decay rate from the environment. The values of the parameter values used are given in Table 3

351

352 From Figure 4, it is evident that the decay of the virus from the environment (Figure 4(b)) which
 353 can be accelerated by disinfecting surfaces reduced the value of \mathcal{R}_0 and consequently the disease
 354 burden. In addition, we observe that an increased proportion of individuals with knowledge of
 355 similar infections from the past that are practising self-protection and preventive measures (see Figure
 356 4(a)) is important in slowing down the infection at the initial stage. Such proportions of individuals
 357 would normally have knowledge about prevention and control mechanisms of the infection just at the
 358 onset of the disease.

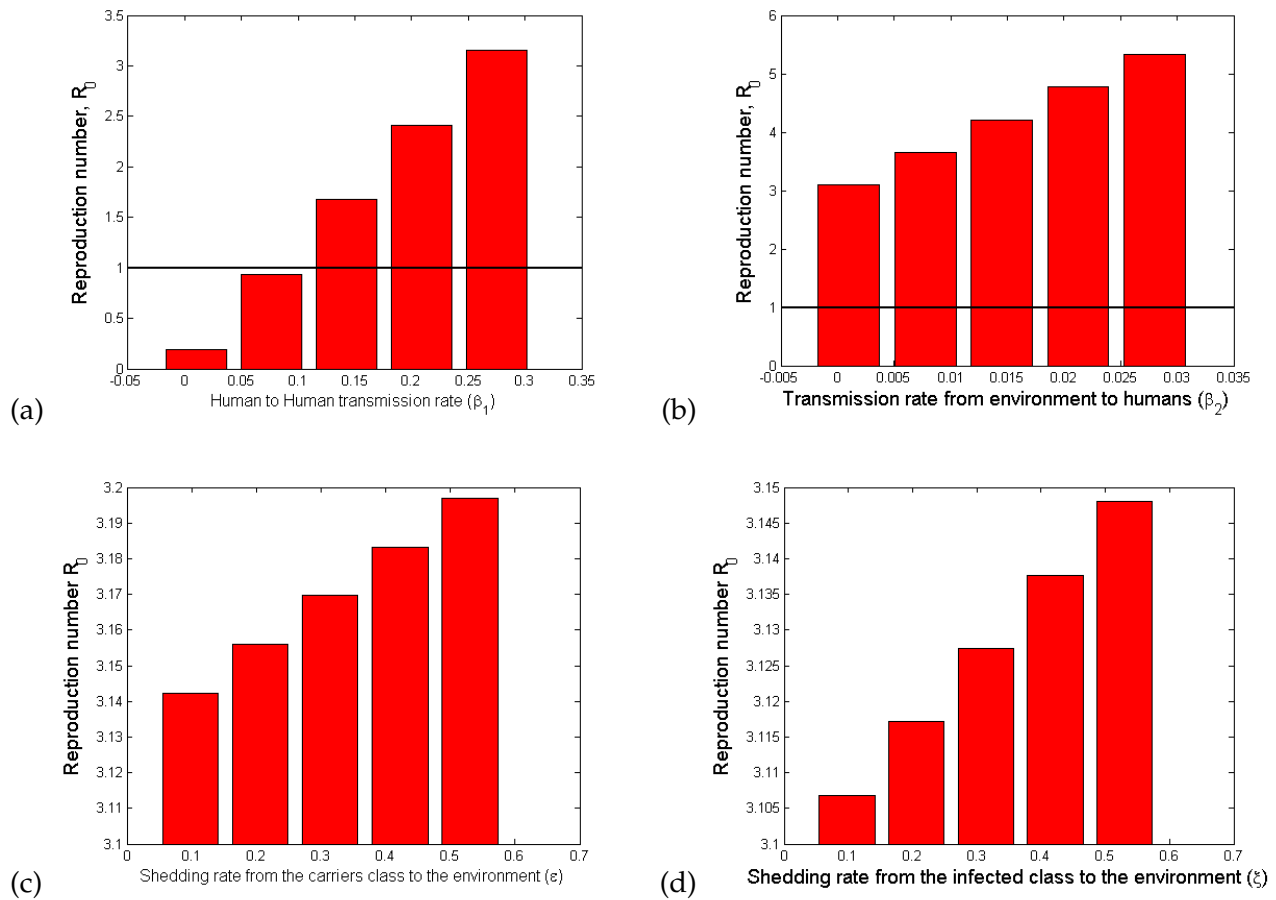


Figure 5: Bar plot showing the effect of the most sensitive parameters to \mathcal{R}_0 : (5(a)) Rate of disease transmission directly from human to human; (5(b)) Rate of disease transmission from the environment; (5(c)) Shedding rate from the carriers class to the environment (ϵ); (5(d)) Shedding rate from the infected class to the environment (ζ). The values of the parameter values used are given in Table 3.

359 We observe in Figure 5 that the increase in person to person contact, β_1 (Figure 5(a)), in poor
360 personal hygiene, β_2 (Figure 5(b)), and in the rate of shedding of the virus into the environment by
361 both carriers (Figure 5(c)) and symptomatic individuals (Figure 5(d)) increases the value of \mathcal{R}_0 and
362 therefore the disease burden. It is evident that the most effective way of containing the infection is
363 by minimizing contact, which is why most cases imposing a lockdown becomes an effective way
364 of slowing the spread of the infection. In addition, good hygiene practices by all individuals are
365 two-fold: (1) avoiding touching surfaces, always washing hands with soap and water, or using alcohol
366 based hand sanitizer, which reduced the likelihood of contracting the pathogen from the environment;
367 (2) those who are sick with symptoms like cough and flu, ought to use masks, when they cough or
368 sneeze, must do so in a sanitary tissue which is then properly disposed off. We also note that hygienic
369 practices without social/physical distancing may not significantly slow down the infection.

370 In summary, we observe that it is possible to reduce the value of \mathcal{R}_0 to a value less than unity
371 by reducing only the value of β_1 below 0.1 (see Figure 5(a)). This observation is in direct agreement
372 with mitigation approaches that are aimed at minimising human-to-human contact (such as social
373 distancing and imposing a lockdown). Therefore, the parameter β_1 is more influential in the model
374 and can also play a significant role in eradication of the disease. The other parameters (see Figures 4,
375 5(b), 5(c) and 5(d)) may reduce the value of \mathcal{R}_0 significantly when applied in combination but not as
376 independent mitigation processes.

377 4.3 Numerical simulations and mitigation strategies

378 There are various ways of intervention mechanisms for COVID-19 that are observed being imple-
379 mented in different part of the world. The strategies differ from country to country depending on
380 the scientific information available to decision makers. For the simulation purpose of this study, we
381 considered five different cases or scenarios of how to apply the interventions. The strategies described
382 in each of the cases below are in addition to the awareness creation for voluntary self-protective
383 mechanisms which are widely communicated through various media outlets. Here, we assume that
384 the average effectiveness of the self-protective measures is 15% (as estimated from the data and
385 reported in Table 3), and the individuals who decided to use any one of them are strict in following
386 the appropriate rules.

387 **Case 1:** In this case, we assume that about 40% of the symptomatic infectious individuals and only
388 1% of the asymptomatic infectious individuals are detected and quarantined. This scenario is
389 based on the assumption that among the people in the I class only about 40% show “above mild”
390 symptoms and hence visit health care facilities, while the remaining individuals in this class
391 (nearly 60% of them) remain at home or at large in the society. Then, through contact tracing
392 mechanisms corresponding the hospitalized individuals, some people will be traced and tested,
393 thereby about 1% of the total asymptomatic individuals can be detected.

394 A similar scenario is being applied currently in some sub-Saharan African countries.

395 The time profile in Figure 6 shows the situation described in Case 1. From this graph we can
396 observe that the infection stabilizes around its endemic equilibrium, which is nearly at 5000
397 cases. (This number depends on the initial conditions and the demographic variables of the
398 population under study.) This shows that the disease persists in the population.

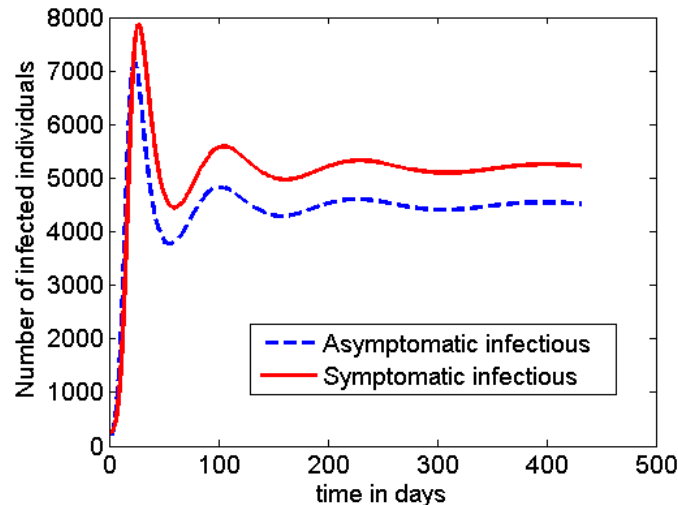


Figure 6: Dynamics of the disease with no additional intervention is applied.

399 **Case 2:** In this case, we assume that strict and longer time (6 weeks) of social distancing rules are
400 enforced by the government nearly 4 weeks after the first positive case of COVID-19 is reported
401 in the community.

402 We assume for simulation purpose that the implementation of the intervention strategy is
403 divided into the following 4 time phases.

404 Phase 1: The first phase, in this case, is 24 days long (measured starting from the first positive
405 case of COVID-19 is reported). During this phase because of lack of information and
406 the nature of the infection, assume (as in Case 1) that only 40% of symptomatic infec-
407 tious individuals and 1% of the asymptomatic infectious individuals are detected and
408 quarantined.

409 phase 2: The second phase is assumed to last for 6 weeks (42 days) in this case. During this
410 period, it is also assumed that

- 411 * 80% of the symptomatic class and 30% of the asymptomatic class are detected and
412 quarantined,
- 413 * a mandatory social distancing rule is imposed, which is assumed to have a 70%
414 reduction of effective contacts of individuals in the society,
- 415 * environmental disinfection is widely carried out, which is assumed to result in a
416 50% reduction in the rate of infection from the environment, and to contribute about
417 the same percent impact in increasing the rate of decay of the pathogen from the
418 environment.

419 Phase 3: The third phase is assumed to be 4 weeks (28 days) long, and is characterised by the
420 partial lift of the 'lockdown' imposed in Phase 2. During this period, it is assumed further
421 that

- 422 * 70% of the symptomatic class and 25% of the asymptomatic class are detected and
423 quarantined,
424 * a relaxed social distancing rule is exercised, which is assumed to have a 25% reduction
425 of effective contacts of individuals in the society,
426 * environmental disinfection is partially carried out, which is assumed to have an impact
427 of reducing the rate of infection from the environment by 30% and increasing the rate
428 of decay of the pathogen from the environment by the same 30%.

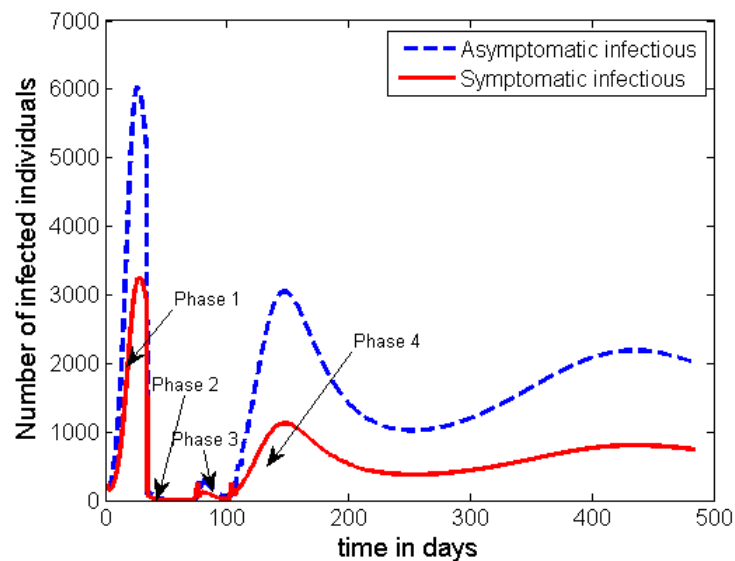


Figure 7: Dynamics of the disease with a mandatory 6-weeks lockdown and a 4-weeks of partial social distancing is imposed as described in Case 1

- 429 Phase 4: The last and fourth phase is the time when the social distancing rule is fully lifted. Due
430 to the lesson learnt from the previous phases, we assume that the following interventions
431 will continue during this period as well
432 * 70% of the I class and 10% of the C class are detected and quarantined,
433 * environmental disinfection is partially carried out, which is assumed to have an impact
434 of reducing the rate of infection from the environment by 20% and increasing the rate
435 of decay of the pathogen from the environment by the same 20%.

436 The time profile of the disease dynamics after implementing the above described interventions
437 strategy is plotted in Figure 7. The figure shows that the count of the infected individuals
438 decreases down to nearly zero in Phases 2 and 3, but the disease returns back into the society
439 soon after. However, the peak of the second wave looks to be much more smaller than the first
440 one. That means, the intervention mechanisms described in the above 4 phases of this case are
441 not enough to contain the disease, and unless some additional intervention mechanisms are
442 developed the disease persists in the society.

443 **Case 3:** In this case, we assume that early action with shorter time social distancing rule is applied.
444 In this scenario, it is assumed that the interventions described in Case 1 started half way
445 through the time Phase 2 was implemented in Case 1. That means, the implementation of the
446 interventions described in the four phases of Case 1 is assumed to be followed, but the length of
447 the time in Phases 1 and 2 is reduced as described below.

- 448 1. Phase 1 lasts only 12 days,
- 449 2. Phase 2 lasts only 3 weeks, and
- 450 3. Phase 3 lasts 4 weeks (the same as in Case 2).

451 Otherwise all the details of the interventions in Case 1 are kept the same. The time profile for
this set of interventions is given in Figure 8. The general behaviour of the graph in Figure 8 is

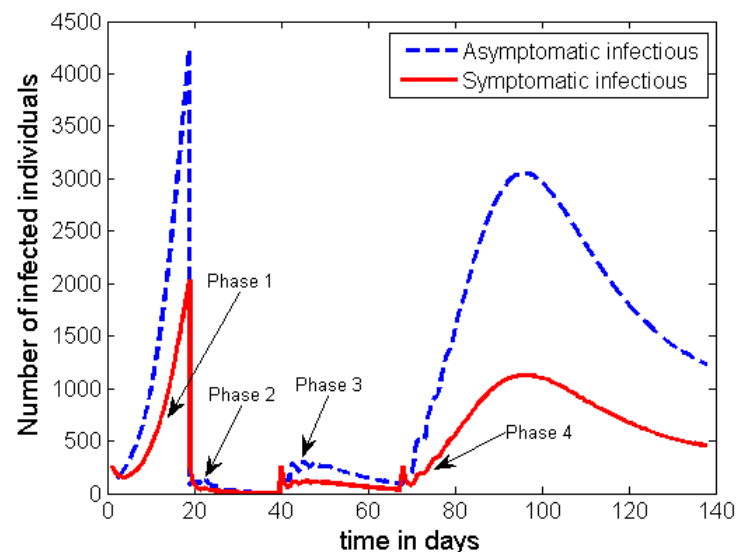


Figure 8: Dynamics of the disease (portraying the scenario in Case 2) with the start of early intervention measures but for half of the time as compared to that of Case 1.

452 the same as that of Figure 7. However, this strategy has an advantage in significantly reducing
453 the height of the first peak. The height of the subsequent peaks are found to be the same unless
454 some additional measures are taken after Phase 3.
455

456 Unfortunately the strategies in both of the above two scenarios (Case 2 and Case 3) do not help
457 to fully contain the disease once it spreads in the population. As can be seen from Figures 7 and
458 8 another wave of outbreak of the disease will emerge at a later stage. Here, we can see that the
459 asymptomatic infectious individuals play the greater role in becoming the major source for the
460 second wave. Therefore, if there is a possibility to track and detect people with asymptomatic
461 infection, and if they can be effectively quarantined for the required period of time there is a
462 possibility for disease to be contained. As it can be observed from Figure 9, if we can increase
463 the effect of detecting and quarantining the asymptomatic individuals to a proportion of about
464 30%, it is possible to significantly reduce the infection to a level that it cannot be a public treat.

465 Otherwise, any lower proportion of this effort will imply the emergence of a second wave of
466 infection in the community.

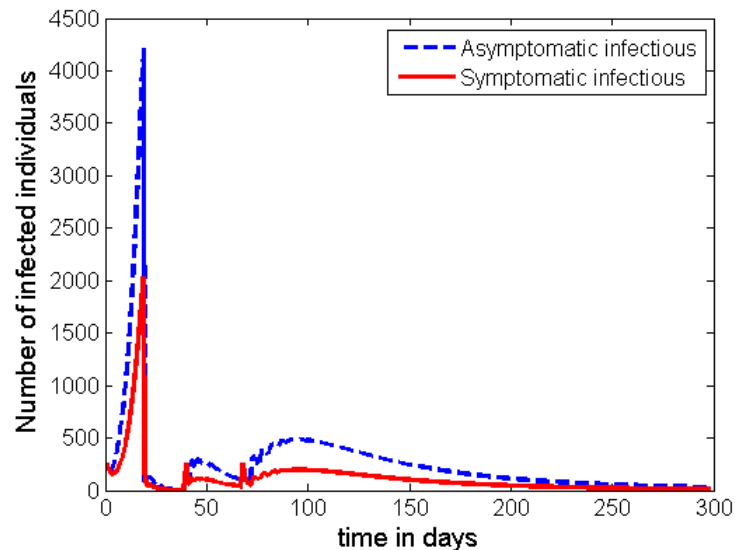


Figure 9: Dynamics of the disease with 30% of the C class and at least 70% of the I class are detected and quarantined in Phase 4 (after the interventions described in Case 2 are carried out).

467 Therefore, to contain COVID-19 in every given community, public health authorities need to
468 work more on the detection and quarantining of the asymptomatic infectious individuals.

469 **Case 4:** In this case, we assume that no lockdown but only large number of testing is applied to
470 detect and quarantine large proportion of infected cases.

471 If it is possible to beef up the effort of tracing the asymptomatic infectious individuals and be
472 able to quarantine at least 35% of them continuously and effectively, our simulation shows that
473 there is a possibility for the disease to be contained without imposing the strict lockdown rule
474 on the total population. The plot in Figure 10 shows the time profile of the count of the infected
475 groups while about 50% of the individuals from I class are effectively quarantined (for example
476 inside appropriate health facilities).

477 We can observe that this intervention strategy can also produce the required result in containing
478 the outbreak as some countries (like South Korea) is currently being following this pattern.

479 **Case 5:** In this case, we assume that the length of the lockdown period is nearly twice to the scenario
480 in Case 2. But the effort in detecting the asymptomatic infectious individuals is kept minimum.
481 This scenario is more applicable in highly resource constrained countries as the current cost of
482 testing is high. In this case, it is assumed that the length of duration for each phase (except for
483 Phase 2) is the same as given in Case 2. However, it is supposed that

- 484 1. the conditions in Phase 1 remains the same,
- 485 2. Phase 2 lasts 11 weeks with 50% of the symptomatic individuals and 5% of the asymp-
486 tomatic individuals are detected and quarantined, while strict social distancing rule with

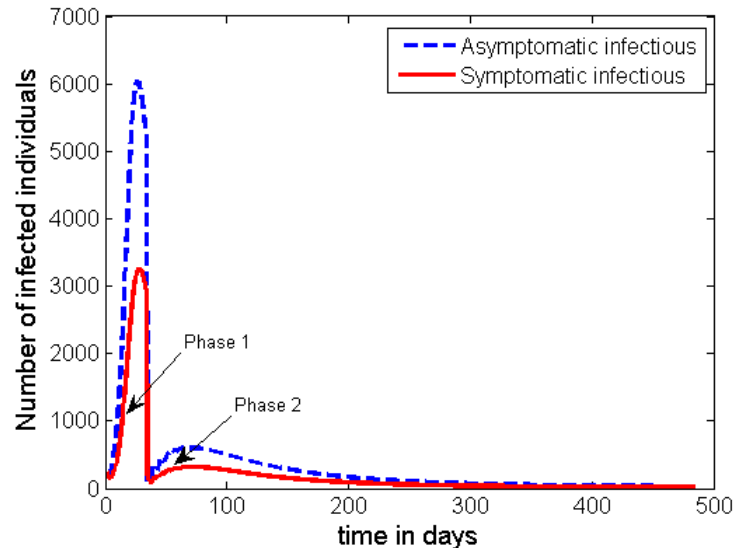


Figure 10: Dynamics of the disease with 30% of the population in the C class and at least 50% of the I class are detected and quarantined just after Phase 1 period.

- 487 an effect of reducing 70% of human contacts and 50% of environmental variables,
- 488 3. Phase 3 lasts 4 weeks (the same as in Case 2), but with 50% of individuals in the I class
- 489 and 10% of individuals in the C class are detected and quarantined, while partial social
- 490 distancing rule with an effect of reducing 25% of human contacts and 25% of environmental
- 491 variables,
- 492 4. Phase 4 continues with detecting and quarantining 50% of members in the I class and 10%
- 493 of members in the C class, while the other mandatory intervention are lifted.

494 The time profile of the infection following the scenario in Case 5 is plotted in Figure 11.

495 The simulation out for this scenario shows that even if we increase the length of lockdown period

496 to 11 weeks (like it was practised in the Hubei province, China) the disease may re-emerge after

497 some period of time. However, the heights of the peaks in the subsequent waves of the disease

498 are much more less than that of the first peak. Therefore, once again, unless the authorities

499 apply some kind of strict contact tracing mechanism and conduct enough testing to detect

500 and isolate up to 30% of the asymptomatic infectious individuals, the disease persist in the

501 community with multiple subsequent waves.

502 In general, from the simulations, we can observe that in all of the above scenarios a transition

503 from one phase to the other intervention phase is characterised by a surge in new cases. However,

504 the number will eventually go down if the intervention in the immediate next phase is effective, and

505 otherwise the disease re-emerges in the population.

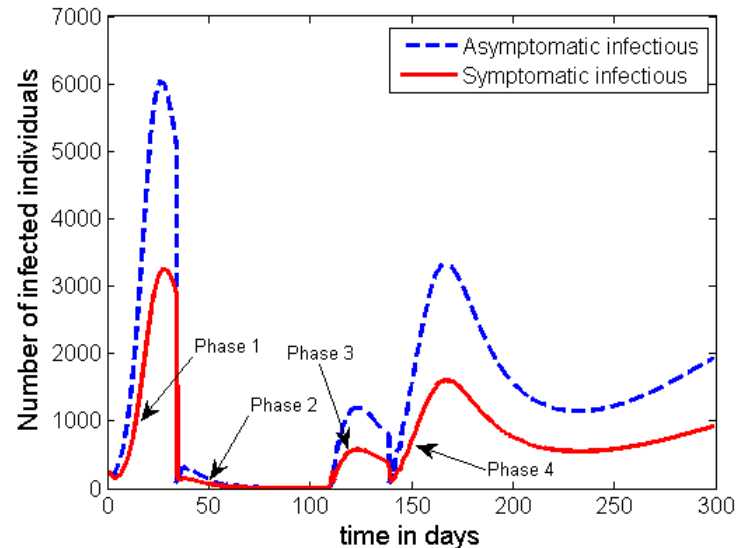


Figure 11: Dynamics of the disease with at most 10% of the population in the C class and at least 50% of the I class are detected and quarantined just after Phase 1 period, with strict social distancing rule imposed for 11 weeks.

506 5 Conclusions

507 We presented a mathematical model for the dynamics of COVID-19 whose first cases were reported
508 in December 2019 in Wuhan-China. The model incorporates a behaviour change function to account
509 for proportion of individuals who decided to use any of the self-protective measures and adhere
510 to it. In addition, it also considers a proportion of individuals with history/knowledge of similar
511 infections from the past and practice necessary protective measures right from the beginning. The
512 model also accounts for asymptomatic carriers of the infection as well as the concentration of the
513 pathogen within the environment. The basic properties of the model including well-posedness, the
514 disease free equilibrium and its stability, model basic reproduction number as well as existence of
515 backward bifurcation were examined. To estimate the parameter values, the model was fitted to the
516 data on daily new cases reported in WHO situation reports 1-57 [43], which accounts for the period
517 from January 21, 2020 to March 17, 2020. From the nominal values from the data fitting, we obtained
518 a reproduction number, $\mathcal{R}_0 \approx 2.9$ (2.1-4) which compares well with the values of \mathcal{R}_0 obtained in other
519 researched, for instance, (2.24 – 3.58) [51] and 3.11(95%CI, 2.39 – 4.13) [34]. From our sensitivity
520 analysis simulations, we observed that for some given parameter combinations the values of \mathcal{R}_0 can
521 be reduced to below 1, and similarly to values much higher than 4.

522 We observed that if the recovering individuals do so with permanent immunity ($\varphi = 0$), then
523 reducing the reproduction number to a value below unity is enough to contain the infection. On the
524 other hand, if recovering individuals do so with temporary immunity ($\varphi \neq 0$), the proposed model
525 exhibits backward bifurcation, which implies that reducing the value of \mathcal{R}_0 below 1 is not enough to
526 contain the infection.

527 By applying the Latin Hypercube sampling scheme, we observed that if the disease is to be
528 easily contained, measures such as; physical/social distancing (which reduces the rate of disease
529 transmission directly from human to human), improved personal hygiene (which reduces the rate of
530 disease transmission from the environment to humans), and minimal shedding of the pathogen into
531 the environment by both asymptomatic and symptomatic individuals, have the greatest potential of
532 slowing the epidemic. We further observed that increased decay of the pathogen from the environment
533 (achieved by disinfecting surfaces) is less significant in reducing/curbing the number of cases.

534 We further observed that having high numbers of people with knowledge from previous similar
535 infections, that are practising the prescribed self-protective measures can delay/slow down the
536 otherwise potentially explosive outbreak. Consequently, the daily number of cases is kept at low
537 manageable levels. In addition, increasing the average effectiveness of the self-protective measures and
538 adherence to such measures is vital in realising low peaks of the number of cases. Furthermore, due to
539 the absence of vaccination or any approved medication, developing capacity to detect carrier groups
540 is very important. From our results, it is recommended that countries should develop capacities to
541 identify and quarantine at least 30% of carriers as well as at least 50% of symptomatic cases if the
542 infection is to be controlled. Our model predicts a possible resurgence of the number of cases if the
543 asymptomatic cases are still many by the time disease spread curbs/lockdown measures are lifted.
544 It is also evident that practising social/physical distancing, good hygiene and disinfecting surfaces
545 to eliminate the virus from surface are vital in reducing the disease burden. But the contribution of
546 disinfecting surfaces is not that high. In addition, we observe from simulations that although disease
547 spread curbs (such as a lockdown measure) may be imposed, their real impact on the number of new
548 cases may only be realised after approximately 21 days, and the reduction (when it appears) could be
549 sharp in the case of a strict lockdown measure with high impact in reducing effective contact between
550 individuals in the population.

551 When providing the mitigation strategies, we did not account for the delay between the actual
552 incidence and the point when cases are confirmed since the actual parameters describing such a delay
553 are not known. In health systems where testing of suspected cases is done after individuals show
554 symptoms or on demand, it is likely to have a big gap between the actual incidence and confirmation
555 of new cases. The impact of the delay between actual incidence and confirmation of case can be
556 explored in future work. In addition, we assumed that all individuals who recover, do so with the
557 same level of immunity. However, this may not necessarily be the case since immunity of individuals
558 is affected by a number of factors including age, cortisol levels and nutrition among others. The
559 impact of differentiated levels of immunity on the disease dynamics and potential resurgence of
560 the epidemic can be explored in the future when relevant data becomes available. Our model did
561 not include the possibility of vaccination or treatment. We however acknowledge their importance
562 in controlling the infection. Therefore, optimal control of infection in presence of these mitigation
563 strategies can be explored in the as some of the relevant data become available.

564 **Acknowledgments.**

565 The authors S.M.K. and H.J.B.N. gratefully acknowledge Botswana International University of Science
566 and Technology (BIUST) that supported their research through the project entitled '*Research Initiation*

567 grant of the office of the DVCRI of BIUST, with grant number DVC/RDI/2/1/161(34).

568 Appendix A – Proof of Theorem 3.1

569 The proof of Theorem 3.1 is outlined here below based on the following two steps.

570 First, we show that all solutions of Eq. (2.2) are nonnegative as required in [3, 37]. To show that
571 the state variables S and S_e of the model are positive for all $t \geq 0$, we use proof by contradiction. We
572 suppose that a trajectory crosses one of the positive cones at times t_1 or t_2 such that:

- 573 • t_1 : $S(t_1) = 0$, $S'(t_1) < 0$, $S_e(t) > 0$, $C(t) > 0$, $I(t) > 0$, $R(t) > 0$, and $E(t) > 0$ for $t \in (0, t_1)$, or
- 574 • t_2 : $S_e(t_2) = 0$, $S'_e(t_2) < 0$, $S(t) > 0$, $C(t) > 0$, $I(t) > 0$, $R(t) > 0$, and $E(t) > 0$ for $t \in (0, t_2)$,

575 Using the first equation of Eq. (2.2), the first assumption leads to

$$S'(t_1) = (1 - h)\pi + (1 - \omega)\varphi R(t_1) > 0,$$

576 which contradicts the first assumption that $S'(t_1) < 0$. Thus, $S(t)$ remains positive for all $t \geq 0$. Here,
577 t_1 is chosen so that our point to be on the positive axis of $S(t)$ so that $R(t_1)$ is positive.

578 Using the second equation of Eq. (2.2),

$$S'_e(t_2) = h\pi + \omega\varphi R > 0,$$

579 which also contradicts the assumption $S'_e(t_2) < 0$. Hence, $S_e(t)$ remains positive for all $t \geq 0$. Based
580 on the third equation of Eq. (2.2),

$$C' = \eta\lambda S + \phi(1 - \rho)\lambda S_e - (\theta + \alpha + \mu)C \geq -(\theta + \alpha + \mu)C, \quad (5.1)$$

581 because $S(t)$ and $S_e(t)$ are nonnegative for $t \geq 0$. Solving Eq. (5.1) yields

$$C(t) \geq C(0) \exp\left(-(\theta + \alpha + \mu)t\right) \geq 0, \quad (5.2)$$

582 Likewise, from the fourth equation of (2.2), we obtain

$$I' = (1 - \eta)\lambda S + (1 - \phi)(1 - \rho)\lambda S_e + \theta C - (\gamma + \mu + \delta)I \geq -(\gamma + \mu + \delta)I. \quad (5.3)$$

583 Solving (5.3) leads to

$$I(t) \geq I(0) \exp\left(-(\gamma + \mu + \delta)t\right) \geq 0. \quad (5.4)$$

584 Similarly, using the last two equations of Eq. (2.2), we have

$$R' = \alpha C + \gamma I - (\varphi + \mu)R \geq -(\varphi + \mu)R, \quad (5.5)$$

585 and

$$E' = \epsilon C + \xi I - \psi E \geq -\psi E, \quad (5.6)$$

586 because $S(t)$, $S_e(t)$, $C(t)$, and $I(t)$ are nonnegative for $t \geq 0$. Solving Eqs. (5.5) and (5.6) gives

$$R(t) \geq R(0) \exp\left(-(\varphi + \mu)t\right) \geq 0, \quad (5.7)$$

587 and

$$E(t) \geq E(0) \exp\left(-\psi t\right) \geq 0, \quad (5.8)$$

588 respectively.

589 Thus, any solution of Eq. (2.2) is nonnegative for $t \geq 0$ and any initial condition in Ω .

590 Finally, the total number of the population $N(t)$ at time t is governed by

$$N'(t) = \pi - \mu N(t) - \delta I \leq \pi - \mu N(t) \quad (5.9)$$

591 Thus, for the initial data $0 \leq N(0) \leq \frac{\pi}{\mu}$, by Gronwall inequality, we obtain

$$0 \leq N(t) \leq \frac{\pi}{\mu}. \quad (5.10)$$

592 Moreover, for the environmental variable E , we have

$$E' = \epsilon C + \zeta I - \psi E \leq (\epsilon + \zeta) \frac{\pi}{\mu} - \psi E, \quad (5.11)$$

593 because $C(t)$ and $I(t)$ are less than $\frac{\pi}{\mu}$ for all $t \geq 0$. Applying again the Gronwall inequality, for

594 $0 \leq E(0) \leq \frac{(\epsilon + \zeta)\pi}{\mu\psi}$, leads into

$$0 \leq E(t) \leq \frac{(\epsilon + \zeta)\pi}{\mu\psi}. \quad (5.12)$$

595 Combining the above two steps and Theorem 2.1.5 in [11] for the existence of unique bounded
596 solution, we infer that any solution of Eq. (2.2) is nonnegative and bounded. Hence, Eq. (2.2) defines
597 a dynamical system on Ω . \square

598 Appendix B: Proof of Theorem 3.3

599 **Proof:** The theorem is the direct application of Theorem 4.1 in [6]. To check the existence of backward
600 bifurcation of the model Eq. (2.2) at $\mathcal{R}_0 = 1$, we use the center manifold theorem [6]. For this purpose,
601 we introduce the following change of variables.

$$x_1 = S, x_2 = S_e, x_3 = C, x_4 = I, x_5 = R, x_6 = E \quad (5.13)$$

so that

$$N = x_1 + x_2 + x_3 + x_4 + x_5, \lambda = \frac{\beta_1(x_4 + \nu x_3)}{N} + \frac{\beta_2 x_6}{x_6 + K}, \text{ and } e(\lambda) = \frac{\lambda^n}{\lambda_0^n + \lambda^n}.$$

602 Moreover, by using the vector notation $X = (x_1, x_2, x_3, x_4, x_5, x_6)^T$, the model Eq. (2.2) can be written
 603 in the form $X'(t) = F = (f_1, f_2, f_3, f_4, f_5, f_6)^T$ as follows:

$$\begin{aligned} x_1' &= (1-h)\pi - (\lambda + \sigma e + \mu)x_1(t) + (1-\omega)\varphi x_6, \\ x_2' &= h\pi + \sigma e x_1 - ((1-\rho)\lambda + \mu)x_2 + \omega\varphi x_5, \\ x_3' &= \eta\lambda x_1 + \phi(1-\rho)\lambda x_2 - k_1 x_3, \\ x_4' &= (1-\eta)\lambda x_1 + (1-\phi)(1-\rho)\lambda x_2 + \theta x_3 - k_2 x_4, \\ x_5' &= \alpha x_3 + \gamma x_4 - k_3 x_5, \\ x_6' &= \epsilon x_3 + \xi x_4 - \psi x_6, \end{aligned} \tag{5.14}$$

604 where,

$$k_1 = \theta + \alpha + \mu, \quad k_2 = \gamma + \mu + \delta, \quad \text{and} \quad k_3 = \varphi + \mu.$$

605 When $\mathcal{R}_0 = 1$ and β_1 is considered as a bifurcation parameter, from (3.5) we get

$$1 = \beta_1 T_1 + T_2 \quad \text{or} \quad \beta_1 = \beta_1^* = \frac{1 - T_2}{T_1}, \tag{5.15}$$

606 where

$$T_1 = \frac{p}{k_1} \left(\nu + \frac{\theta}{k_2} \right) + \frac{q}{k_2} \quad \text{and} \quad T_2 = \frac{\beta_2 \pi}{\mu \psi K} \left[\frac{p}{k_1} \left(\epsilon + \frac{\theta \xi}{k_2} \right) + \frac{q \xi}{k_2} \right].$$

607 Further more, $\beta_1 < \beta_1^*$ if and only if $\mathcal{R}_0 < 1$ and $\beta_1 > \beta_1^*$ whenever $\mathcal{R}_0 > 1$.

608 The Jacobian of the system (5.14) at the associated DFE (\mathcal{E}_0) is

$$J(\mathcal{E}_0) = \begin{pmatrix} -\mu & 0 & -\nu\beta_1^*(1-h) & -\beta_1^*(1-h) & (1-\omega)\varphi & -\frac{\beta_2(1-h)\pi}{\mu K} \\ 0 & -\mu & -(1-\rho)h\nu\beta_1^* & -(1-\rho)h\beta_1^* & \omega\varphi & -\frac{(1-\rho)h\beta_2\pi}{\mu K} \\ 0 & 0 & p\nu\beta_1^* - k_1 & p\beta_1^* & 0 & \frac{p\beta_2\pi}{\mu K} \\ 0 & 0 & q\nu\beta_1^* + \theta & q\beta_1^* - k_2 & 0 & \frac{q\beta_2\pi}{\mu K} \\ 0 & 0 & \alpha & \gamma & -k_3 & 0 \\ 0 & 0 & \epsilon & \xi & 0 & -\psi \end{pmatrix}, \tag{5.16}$$

609 where $p = \eta(1-h) + \phi(1-\rho)h$, and $q = (1-\eta)(1-h) + (1-\phi)(1-\rho)h$.

610 The transformed system Eq. (5.14), with $\beta_1 = \beta_1^*$, has a non-hyperbolic equilibrium point such
 611 that the linear system has a simple eigenvalue with zero real part and all other eigenvalues have
 612 negative real parts. Hence, the centre manifold theory [6] can be used to analyse the dynamics of the
 613 model Eq. (5.14) near $\beta_1 = \beta_1^*$. By using the notation in [6], the following computations are carried
 614 out.

615 The right-eigenvector

$$w = (w_1, w_2, w_3, w_4, w_5, w_6)^T \tag{5.17}$$

616 associated with the zero eigenvalue of $J(\mathcal{E}_0)$ such that

$$J(\mathcal{E}_0).w = 0$$

617 at $\beta_1 = \beta_1^*$ is given by

$$\begin{aligned} w_1 &= Dw_3, \quad w_2 = Gw_3, \quad w_3 = w_3 > 0, \\ w_4 &= Aw_3, \quad w_5 = \frac{1}{k_3}(\alpha + \gamma A)w_3, \quad w_6 = \frac{1}{\psi}(\epsilon + \zeta A)w_3, \end{aligned}$$

618 where

$$\begin{aligned} A &= \frac{\mu\psi k_1 K \left[\beta_1^* \left(\frac{p\theta}{k_1 k_2} + \frac{q}{k_2} \right) + \frac{\beta_2 \pi}{\mu\psi K} \left(\frac{p\theta\zeta}{k_1 k_2} + \frac{q\zeta}{k_2} \right) \right]}{p(\mu\psi\beta_1^* K + \zeta\beta_2 \pi)} > 0, \\ D &= \frac{1}{\mu} \left[\frac{(1-\omega)\varphi(\alpha + \gamma A)}{k_3} - (1-h) \left(\beta_1^*(\nu + A) + \frac{\beta_2 \pi}{\mu\psi K}(\epsilon + \zeta A) \right) \right], \\ G &= \frac{1}{\mu} \left[\frac{\omega\varphi}{k_3}(\alpha + \gamma A) - (1-\rho)h \left(\beta_1^*(\nu + A) + \frac{\beta_2 \pi}{\mu\psi K}(\epsilon + \zeta A) \right) \right]. \end{aligned} \quad (5.18)$$

619 Similarly, the left-eigenvector

$$v = (v_1, v_2, v_3, v_4, v_5, v_6), \quad (5.19)$$

620 of $J(x^*)$ such that

$$v.J(\mathcal{E}_0) = 0$$

621 associated with the zero eigenvalue is given by,

$$\begin{aligned} v_1 &= 0, \quad v_2 = 0, \quad v_3 = v_3 > 0, \\ v_4 &= Fv_3, \quad v_5 = 0, \quad v_6 = \frac{\beta_2 \pi}{\mu\psi K}(p + qF)v_3, \end{aligned}$$

622 where

$$F = \frac{p(\mu\psi\beta_1^* K + \zeta\beta_2 \pi)}{q(\nu\mu\psi\beta_1^* K + \epsilon\beta_2 \pi) + \mu\psi\theta K} A > 0.$$

623 The right-eigenvector w and the left-eigenvector v need to satisfy the condition $v.w = 1$.

624 The bifurcation coefficient a at the DFE (\mathcal{E}_0) is given by

$$\begin{aligned} a &= \sum_{k,i,j=1}^6 v_k w_i w_j \frac{\partial^2 f_k}{\partial x_i \partial x_j}(\mathcal{E}_0, \beta_1^*), \\ &= \sum_{i,j=1}^6 \left[v_3 w_i w_j \frac{\partial^2 f_3}{\partial x_i \partial x_j}(\mathcal{E}_0, \beta_1^*) + v_4 w_i w_j \frac{\partial^2 f_4}{\partial x_i \partial x_j}(\mathcal{E}_0, \beta_1^*) + v_6 w_i w_j \frac{\partial^2 f_6}{\partial x_i \partial x_j}(\mathcal{E}_0, \beta_1^*) \right] \\ &= 2 \left\{ D \left[\frac{\mu\beta_1}{\pi}(\nu + A) \left(\eta - p + F(1 - \eta - q) \right) + \frac{\beta_2(\epsilon + \zeta A)}{\psi K} \left(\eta + F(1 - \eta) \right) \right] \right. \\ &+ G \left[\frac{\mu\beta_1}{\pi}(\nu + A)(1 - h) \left[\left(-\eta + \phi(1 - \rho) \right) + F \left(-(1 - \eta) + (1 - \phi)(1 - \rho) \right) \right] \right. \\ &+ \left. \left. \frac{(1 - \rho)\beta_2(\epsilon + \zeta A)}{\psi K} \left(\phi + F(1 - \phi) \right) \right] \right. \\ &- \left. (p + qF) \left[\frac{\mu\beta_1}{\pi} \left(\nu + A(1 + \nu + A) + \frac{\alpha + \gamma A}{k_3}(\nu + A) \right) + \frac{(\epsilon + \zeta A)^2}{\mu\psi^2 K^2} \beta_2 \pi \right] \right\} v_3 w_3^2 \end{aligned} \quad (5.20)$$

625

626 Thus, the bifurcation coefficient a , can be positive for the right choice of the parametric values that
627 satisfy the condition in Eq. (3.6).

628 The second bifurcation coefficient b is given by

$$\begin{aligned} b &= \sum_{k,j=1}^6 v_k w_j \frac{\partial^2 f_k}{\partial x_j \partial \beta_1}(\mathcal{E}_0, \beta_1^*), \\ &= \sum_{j=1}^6 \left[v_3 w_j \frac{\partial^2 f_3}{\partial x_j \partial \beta_1}(\mathcal{E}_0, \beta_1^*) + v_4 w_j \frac{\partial^2 f_4}{\partial x_j \partial \beta_1}(\mathcal{E}_0, \beta_1^*) + v_6 w_j \frac{\partial^2 f_6}{\partial x_j \partial \beta_1}(\mathcal{E}_0, \beta_1^*) \right] \\ &= (v + A)(p + qF)v_3 w_3 \end{aligned} \tag{5.21}$$

629 Clearly, $b > 0$ because A and F are positive.

630 When $\varphi = 0$, D and G in (5.18) are negative and a in (5.20) is negative as well. Hence, by Theorem
631 4.1 in [6], the model will not exhibit a backward bifurcation at $\mathcal{R}_0 = 1$.

632 References

- 633 [1] Blower, S.M., Dowlatabadi, H.: Sensitivity and uncertainty analysis of complex models of disease
634 transmission: An HIV model as an example. *Int. Stat. Rev* **62**, 229–243 (1994)
- 635 [2] Buonomo, B.: Effects of information-dependent vaccination behavior on coronavirus outbreak:
636 *insights from a SIRI model*. Submitted to: *Ricerche di Matematica* (Accessed on March 2, 2020)
- 637 [3] Busenberg, S., Cooke, K.: Vertically Transmitted Disease: *Models and Dynamics*, vol. 23. Springer-
638 Verlag (1993)
- 639 [4] Business-Insider: A day-by-day breakdown of coronavirus symptoms shows how
640 the disease COVID-19 goes from bad to worse (Accessed on April 8, 2020).
641 <https://www.businessinsider.com/coronavirus-covid19-day-by-day-symptoms-patients-2020-2>
- 642 [5] Camacho, A., Kucharski, A., Aki-Sawyer, Y., et al: Temporal changes in ebola transmission in
643 sierra leone and implications for control requirements: *a real-time modelling study*. *PLoS Curr* **7**
644 (2015)
- 645 [6] Castilo-Chavez, C., Song, B.: Dynamical models of tuberculosis and their application. *Mathemat-*
646 *ical Biosciences and Engineering* **1**(2), 361 – 404 (2004)
- 647 [7] CDC: Symptoms of coronavirus (Accessed on April 8, 2020).
648 <https://www.cdc.gov/coronavirus/2019-ncov/symptoms-testing/symptoms.html>
- 649 [8] Chan, J.F., Yuan, S., Kok, K.H., To, K.K., Chu, H., Yang, J., Xing, F., Liu, J., Yip, C.C., Poon, R.W.,
650 Tsoi, H.W., Lo, S.K., Chan, K.H., Poon, V.K., Chan, W.M., Ip, J.D., Cai, J.P., Cheng, V.C., Chen, H.,
651 Hui, C.K., Yuen, K.Y.: A familial cluster of pneumonia associated with the 2019 novel coronavirus
652 indicating person-to-person transmission: *A study of a family cluster*. *Lancet* **395**, 514–523 (2020)

- 653 [9] Chen, T.M., Rui, J., Wang, Q.P., Zhao, Z.Y., Cui, J.A., Yin, L.: A mathematical model for simulating
654 the phase-based transmissibility of a novel coronavirus. *Infectious Disease of Poverty* **9**, 24 (2020).
655 DOI 10.1186/s40249-020-00640-3
- 656 [10] China-CDC: Vital surveillances: The epidemiological characteristics of an outbreak
657 of 2019 novel coronavirus diseases (COVID-19)–China 2020 (2020). Found at
658 <http://weekly.chinacdc.cn/en/article/id/e53946e2-c6c4-41e9-9a9bfea8db1a8f51>
- 659 [11] Diekmann, O., Heesterbeek, J.: *Mathematical Epidemiology of Infectious Diseases*. Wiley (2000)
- 660 [12] Djidjou-Demassea, R., Michalakisa, Y., Choisy, M., Sofoneaa, M.T., Alizon, S.: Optimal COVID-
661 19 epidemic control until vaccine deployment. medRxiv: preprint (Accessed on April 8, 2020).
662 DOI 10.1101/2020.04.02.20049189
- 663 [13] d’Onofrio, A., Manfredi, P., Salinelli, E.: Vaccinating behaviour, information, and the dynamics of
664 SIR vaccine preventable diseases. *Theoretical Population Biology* **71**, 301 – 317 (2007)
- 665 [14] Funk, S., Gilad, E., Jansen, V.A.: Endemic disease, awareness, and local behavioural response. *J.*
666 *Theor. Biol.* **264**, 501 – 509 (2010)
- 667 [15] Funk, S., Salathé, M., Jansen, V.A.A.: Modelling the influence of human behaviour on the spread
668 of infectious diseases: *a review*. *J. R. Soc. Interface* **7**, 1247 – 1256 (2010)
- 669 [16] Gaun, W., Ni, Z., *et. al.*: Clinical characteristics of 2019 novel coronavirus infection in china.
670 MedRxiv: preprint p. 30 pages (2020)
- 671 [17] Hatzopoulos, V., Taylor, M., Simon, P.L., Kiss, I.Z.: Multiple sources and routes of information
672 transmission: *implications for epidemic dynamics*. *Math. Biosci.* **231**, 197 – 209 (2011)
- 673 [18] Heneghan, C., Brassey, J., Jefferson, T.: COVID-19: What proportion are asymptomatic?
674 (Accessed on April 9, 2020). [https://www.cebm.net/covid-19/covid-19-what-proportion-are-](https://www.cebm.net/covid-19/covid-19-what-proportion-are-asymptomatic/)
675 [asymptomatic/](https://www.cebm.net/covid-19/covid-19-what-proportion-are-asymptomatic/)
- 676 [19] Hoare, A., Regan, D.G., Wilson, D.P.: Sampling and statistical analyses tools (SaSAT) for
677 computational modelling. *Math. Biosci.* **5** (2008). DOI 10.1186/1742-468-5-4
- 678 [20] Huang, C., Wang, Y., Li, X., *et. al.*: Clinical features of patients infected with 2019 novel coronavirus
679 in Wuhan, China. *Lancet* **395**, 497–506 (2020)
- 680 [21] Isaacs, D., Flowers, D., Clarke, J.R., Valman, H.B., MacNaughton, M.R.: Epidemiology of
681 coronavirus respiratory infections. *Arch. dis. child.* **58**, 500–503 (1983)
- 682 [22] Juher, D., Kiss, I.Z., na, J.S.: Analysis of an epidemic model with awareness decay on regular
683 random networks. *J. Theor. Biol.* **365**, 457 – 468 (2015)
- 684 [23] Kamgang, J.C., Sallet, G.: Computation of threshold conditions for epidemiological models and
685 global stability of the disease-free equilibrium (DFE). *Mathematical Biosciences* **213**, 1–12 (2008)
- 686 [24] Kassa, S.M., Ouhinou, A.: Epidemiological models with prevalence dependent endogenous
687 self-protection measure. *Math. Biosci.* **229**, 41 – 49 (2011)
- 688 [25] Kassa, S.M., Ouhinou, A.: The impact of self-protective measures in the optimal interventions for
689 controlling infectious diseases of human population. *J Math Biol.* **70**, 213 – 236 (2015)

- 690 [26] Kassa, S.M., Workineh, Y.H.: Effect of negligence and length of time delay in spontaneous
691 behavioural changes for the response to epidemics. *Math Meth Appl Sci.* **41**, 8613 – 8635 (2018).
692 DOI 10.1002/mma.4926
- 693 [27] Khan, M.A., Atangana, A.: Modeling the dynamics of novel coronavirus (2019-nCov) with
694 fractional derivative. *Alexandria Engineering Journal In Press* (2020)
- 695 [28] Kucharski, A.J., Russell, T.W., Diamond, C., Liu, Y., Edmunds, J., Funk, S., et al: Early dynamics
696 of transmission and control of COVID-19: *a mathematical modelling study*. *Lancet Infect Dis* (2020).
697 DOI 10.1016/S1473-3099(20)30144-4
- 698 [29] Kumar, A., Srivastava, P.K., Takeuchi, Y.: Modeling the role of information and limited optimal
699 treatment on disease prevalence. *Journal of Theoretical Biology* **414**, 103 – 119 (2017)
- 700 [30] Layne, S.P., Hyman, J.M., Morens, D.M., Taubenberger, J.K.: New coronavirus outbreak:
701 Framing questions for pandemic prevention. *Sci. Transl. Med.* **12**, eabb1469 (2020). DOI
702 10.1126/scitranslmed.abb1469
- 703 [31] Macrotrends: China Life Expectancy 1950-2020 (Accessed on April 9, 2020).
704 <https://www.macrotrends.net/countries/CHN/china/life-expectancy>
- 705 [32] Manfredi, P., d’Onofrio, A.: *Modeling the Interplay between Human Behavior and the Spread of*
706 *Infectious Diseases*. Springer, New York (2013)
- 707 [33] NHS: SARS (Severe Acute Respiratory Syndrome) (Accessed on April 13, 2020). Available from
708 <https://www.nhs.uk/conditions/sars/>
- 709 [34] Read, J.M., Bridgen, J.R.E., Cummings, D.A.T., Ho, A., Jewell, C.P.: Novel coronavirus 2019-nCoV:
710 early estimation of epidemiological parameters and epidemic predictions. *MedRxiv: preprint*
711 (2020). DOI 10.1101/2020.01.23.20018549
- 712 [35] Riley, S., Fraser, C., Donnelly, C.A., et al: Transmission dynamics of the etiological agent of SARS
713 in Hong Kong: *impact of public health interventions*. *Science* **300**, 1961 – 66 (2003)
- 714 [36] Sameni, R.: Mathematical modeling of epidemic diseases: A case study of the COVID-19
715 coronavirus. *arXiv: preprint* (Accessed on April 2, 2020). DOI <http://arxiv.org/abs/2003.11371v1>
- 716
- 717 [37] Stuart, A.M., Humphries, A.R.: *Dynamical Systems and Numerical Analysis*. Cambridge
718 University Press, Cambridge (1998)
- 719 [38] van den Driessche, P., Watmough, J.: Reproduction numbers and sub-threshold endemic equi-
720 libria for compartmental models of disease transmission. *Mathematical Biosciences* **180**, 29–48
721 (2002)
- 722 [39] van Doremalen, N., Bushmaker, T., Morris, D.H., Holbrook, M.G., Gamble, A., Williamson, B.N.,
723 Tamin, A., Harcourt, J.L., Thornburg, N.J., Gerber, S.I., Lloyd-Smith, J.O., de Wit, E., Munster, V.J.:
724 Aerosol and surface stability of SARS-CoV-2 as compared with SARS-CoV-1. *The New England*
725 *Journal of Medicine* **March 17**, 1–3 (2020). DOI 10.1056/NEJMc2004973
- 726 [40] Wang, Z., Bauch, C.T., Bhattacharyya, S., d’Onofrio, A., Manfredi, P., Perc, M., Perra, N., Salathé,
727 M., Zhao, D.: Statistical physics of vaccination. *Physics Reports* **664**, 1 – 113 (2016)

- 728 [41] WHO: Middle East Respiratory Syndrome: MERS situation update, January 2020 (Accessed
729 on April 13, 2020). Available from [http://www.emro.who.int/health-topics/mers-cov/
730 mers-outbreaks.html](http://www.emro.who.int/health-topics/mers-cov/mers-outbreaks.html)
- 731 [42] WHO: Coronavirus disease 2019 (COVID-19): Situation Report-46 (Accessed on April 8,
732 2020). [https://www.who.int/docs/default-source/coronaviruse/situation-reports/20200306-
733 sitrep-46-covid-19.pdf?sfvrsn=96b04adf_2](https://www.who.int/docs/default-source/coronaviruse/situation-reports/20200306-sitrep-46-covid-19.pdf?sfvrsn=96b04adf_2)
- 734 [43] WHO: Coronavirus disease (COVID-2019) situation reports (Accessed on April 8, 2020).
735 <https://www.who.int/emergencies/diseases/novel-coronavirus-2019/situation-reports>
- 736 [44] WHO: Total population, life expectancy and ethnicity of hubei (Accessed on March 28, 2020).
737 Available from <http://www.china.org.cn/english/features/66665.htm>
- 738 [45] Wölfel, R., Corman, V.M., Guggemos, W., Seilmaier, M., Zange, S., Müller, M.A., Niemeyer,
739 D., Kelly, T.C.J., Vollmar, P., Rothe, C., Hoelscher, M., Bleicker, T., Brünink, S., Schneider, J.,
740 Ehmann, R., Zwirgmaier, K., Drosten, C., Wendtner, C.: Virological assessment of hospitalized
741 cases of coronavirus disease 2019. medRxiv: preprint (Accessed on April 2, 2020). DOI
742 10.1101/2020.03.05.20030502
- 743 [46] Wong, T.: Coronavirus: Why some countries wear face masks and others don't. BBC News
744 (Accessed on March 26, 2020). Available from <https://www.bbc.com/news/world-52015486>
- 745 [47] Worldometer: Coronavirus Incubation Period (Accessed on March 29, 2020). Available from
746 <https://www.worldometers.info/coronavirus/coronavirus-incubation-period/>
- 747 [48] Worldometers: COVID-19 Coronavirus Pandemic (Accessed on April 9,
748 2020). Available from [https://www.worldometers.info/coronavirus/?fbclid=
749 IwAR20hpWiFATgR5aenmpd2KHJOEIi89WgIHqGEts5TuDlnTTGUU6Liq1kbp4](https://www.worldometers.info/coronavirus/?fbclid=IwAR20hpWiFATgR5aenmpd2KHJOEIi89WgIHqGEts5TuDlnTTGUU6Liq1kbp4)
- 750 [49] Wu, J.T., Leung, K., Leung, G.M.: Nowcasting and forecasting the potential domestic and
751 international spread of the 2019-nCoV outbreak originating in wuhan, china: *a modelling study*.
752 *Lancet* (2020). DOI 10.1016/S0140-6736(20)30260-9
- 753 [50] Wu, L.P., Wang, N.C., Chang, Y.H., Tian, X.Y., Na, D.Y., Zhang, L.Y., Zheng, L., Lan, T., Wang, L.F.,
754 Liang, G.D.: Duration of antibody responses after severe acute respiratory syndrome. *Emerging*
755 *infectious disease* **13**(10), 1562 (2007)
- 756 [51] Zhao, S., Lin, Q., Ran, J., Musa, S., Yang, G., Wang, W., Lou, Y., Gao, D., Yang, L., He, D., Wang,
757 M.: Preliminary estimation of the basic reproduction number of novel coronavirus (2019-nCoV) in
758 China, from 2019 to 2020: A data-driven analysis in the early phase of the outbreak. *International*
759 *Journal of Infectious Diseases* **92**, 214–217 (2020)